Spin Fluctuations in Sr_2RuO_4 from Polarized Neutron Scattering: Implications for Superconductivity

P. Steffens,[1,2] Y. Sidis,[3] J. Kulda,[2] Z. Q. Mao,[4,5,6] Y. Maeno,[4] I. I. Mazin,[7] and M. Braden[1,*]
[1]*II. Physikalisches Institut, Universität zu Köln, Zülpicher Str. 77, D-50937 Köln, Germany*
[2]*Institut Laue Langevin, 71 avenue des Martyrs, 38000 Grenoble, France*
[3]*Laboratoire Léon Brillouin, C.E.A./C.N.R.S., F-91191 Gif-sur-Yvette CEDEX, France*
[4]*Department of Physics, Graduate School of Science, Kyoto University, Kyoto 606-8502, Japan*
[5]*Department of Physics, Tulane University, New Orleans, Louisiana 70118, USA*
[6]*Department of Physics, Pennsylvania State University, University Park, Pennsylvania 16802, USA*
[7]*Code 6393, Naval Research Laboratory, Washington, DC 20375, USA*

(Received 9 July 2018; published 1 February 2019)

Triplet pairing in Sr_2RuO_4 was initially suggested based on the hypothesis of strong ferromagnetic spin fluctuations. Using polarized inelastic neutron scattering, we accurately determine the full spectrum of spin fluctuations in Sr_2RuO_4. Besides the well-studied incommensurate magnetic fluctuations, we do find a sizable quasiferromagnetic signal, quantitatively consistent with all macroscopic and microscopic probes. We use this result to address the possibility of magnetically driven triplet superconductivity in Sr_2RuO_4. We conclude that, even though the quasiferromagnetic signal is stronger and sharper than previously anticipated, spin fluctuations alone are not enough to generate a triplet state strengthening the need for additional interactions or an alternative pairing scenario.

DOI: 10.1103/PhysRevLett.122.047004

Superconducting Sr_2RuO_4 [1–3] was proposed to be a solid-state analog of He^3, i.e., a triplet superconductor [4,5], based on its proximity to $SrRuO_3$, a ferromagnetic (FM) metal. A simple model derived from the density-functional theory (DFT) for $SrRuO_3$, $CaRuO_3$, and $SrYRu_2O_6$ [6] ascribed the mass and spin susceptibility renormalization to FM fluctuations, and predicted a triplet pairing [5]. Experimental evidence pointing toward a particular (chiral-p) triplet was obtained, such as temperature-independent uniform susceptibility for the in-plane fields and time-reversal symmetry breaking [2,7–9]. However, the dominant spin fluctuations in Sr_2RuO_4 are not FM (i.e., $q = 0$), but incommensurate (IC) antiferromagnetic (AFM) [10,11] and several experiments are inconsistent with either triplet states, or time-reversal breaking, or both [9]. Various theories were proposed to explain triplet pairing by incorporating higher-order vertex corrections [12,13], the interplay of incommensurate charge and spin fluctuations [14] or orbital fluctuations [15,16], arriving at different superconducting (SC) states. Even the question about which bands drive pairing remains controversial [17,18].

The Fermi surface of Sr_2RuO_4 is known to tiny details [2,19–21]. It has two quasi-one-dimensional (Q1D), and one rather isotropic quasi-two-dimensional (Q2D) sheets, derived from $d_{xz,yz}$ and d_{xy} orbitals, respectively. Sr_2RuO_4 exhibits an almost temperature independent normal-state susceptibility [22], which is enhanced by a factor ~7 compared to the DFT value [23–25]. The enhancement factor of the IC fluctuations is even larger, ~30 [11,26,27], since the bare susceptibility is larger [10]. Also the electronic specific heat coefficient of about 38 $\mathrm{mJ/mol\,K^2}$ is enhanced by a factor of ~3, yielding a Wilson ratio of ~2. Similarly, quantum oscillations show strong and band-dependent mass renormalizations, which can be explained by quasiferromagnetic (QFM) fluctuations [5], in the spirit of He^3, but also in terms of local Hund's rule fluctuations [28,29].

Inelastic neutron scattering (INS) experiments detect strong IC spin fluctuations at $\mathbf{q}_{\mathrm{IC}} = (\pm 0.3, \pm 0.3, q_l)$ [11,26,27,30–33] arising from nesting in the Q1D bands. Upon minor substitution with Ti or Ca, this instability condenses into a static spin-density wave with the same $\mathbf{Q}$ [34–37]. INS also assesses the anisotropy of magnetic excitations, which is known to favor triplet pairing [38–40], and find it to be non-negligible, but still small [30]. Finally, recent high-resolution INS reveals that the nesting fluctuations do not change between the normal and superconducting states even for energies well below the SC gap [33]. The NMR relaxation rate, $1/T_1T$, probes the spin susceptibility $\chi''(\mathbf{q},\omega)/\omega$ integrated over the entire Brillouin zone, and exhibits the same temperature dependence as the INS nesting signal [11,26,41,42], indicating that it is dominated by the latter. However, $1/T_1T$ also shows a weaker, temperature-independent offset, pointing to another contribution tentatively attributed to the FM response. This tendency towards ferromagnetism can be enhanced by Co [43] or Ca [44] substitution.

To this end, we have used polarized INS to search for the missing FM fluctuations in Sr_2RuO_4. The magnetic

response consists of two components: a broad maximum around $\mathbf{q} = 0$, which we will call QFM, and an IC, and much stronger, AFM component. We entered this full magnetic susceptibility into the BCS equations describing spin-fluctuation-induced SC pairing.

Because neutron polarization analysis suffers from a reduced intensity, we used a large sample of ten aligned crystals grown at Kyoto University [45] with a total volume of 2.2 cm^3 and a mosaic spread of 1.9(2) degrees. Experiments were performed on the spectrometer IN20 at the Institut Laue Langevin, for details see the Supplemental Material [46]. In general, neutron scattering only senses magnetic components that are polarized perpendicular to the scattering vector $\mathbf{Q}$. The polarization analysis distinguishes spin-flip (SF_i with $i = x$, y, and z the direction of neutron polarization) and non-spin-flip (NSF_i) processes and adds further selection rules. Phonon scattering and nuclear Bragg peaks only contribute to the NSF_i channels, but magnetic scattering contributes to the SF_i channel when the magnetic component is perpendicular to the direction of neutron polarization, and to the NSF_i channel otherwise. We use the conventional coordinate system with $\mathbf{x}$ parallel to $\mathbf{Q}$, $\mathbf{z}$ perpendicular to the scattering plane, and $\mathbf{y} = \mathbf{z} \times \mathbf{x}$.

Even with our large sample it was impossible to quantitatively analyze the QFM response by unpolarized INS, because it is too little structured in $\mathbf{q}$ space impeding a background (BG) determination, see Supplemental Material [46]. In contrast, the polarization analysis permits a direct BG subtraction at each point in $\mathbf{Q}$ and energy. For instance, $2I(SF_x)$-$I(SF_y)$-$I(SF_z)$ yields a BG-free total magnetic signal (up to a correction for the finite flipping ratio). Figures 1(b) and 1(c) show a representative scan through both the IC and the FM $\mathbf{Q}$ positions. The full polarization analysis is shown for the SF (b) and the NSF (c) channels. The SF signals have been counted with better statistics, because the SF count rates always contain the magnetic signal and have a lower BG. Only the NSF_y and NSF_z channels contain a single magnetic component superposed with the larger NSF scattering, which contains all the phonon contributions. The appearance of the nesting signal in various channels is well confirmed; Fig. 1(b) clearly shows the anisotropy of the IC nesting signal at $(-0.3, 0.7, 0)$ discussed in Ref. [30]. The sharp enhancement at (0,1,0) is present only in the NSF channel, which proves its nonmagnetic character (the longitudinal zone-boundary phonon) [47,48]. The finite flipping ratio was determined on several phonon modes, which integrates the signal of all individual crystals, yielding values between 8 and 10. The final analysis only used the SF data, corrected by the average flipping ratio, because of their higher signal to BG ratio [49].

Polarized INS results displaying the average of two magnetic components (in plane plus out of plane) are shown in Fig. 1 for $T = 1.6$ K and in the Supplemental Material for $T = 150$ K [46]. In order to compare scans taken at different but equivalent scattering vectors, a correction for the magnetic form factor has been applied. The observation of magnetic fluctuations in so many different scans unambiguously documents the existence of sizeable QFM fluctuations. The analysis furthermore yields the absolute scale of the magnetic response throughout the entire Brillouin zone, which allows us to construct a model for the full susceptibility $\chi''(\mathbf{q}, E)$. The calibration into absolute susceptibility units has been performed by the comparison with the scattering intensity arising from an acoustic phonon, similar to the procedure described in Ref. [50]. This calibration can be performed with high precision in the case of Sr_2RuO_4, because the phonon

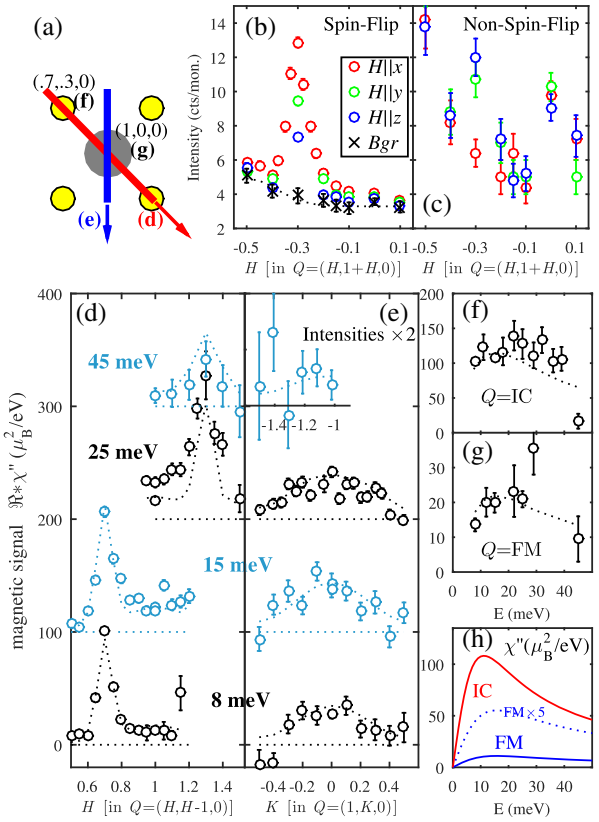

FIG. 1. (a) 2D reciprocal space of Sr_2RuO_4; QFM scattering is indicated by large (gray) discs and the IC signal by small (yellow) circles. Arrows show typical scan directions. (b)–(c) Diagonal scans at 8 meV and 1.6 K [across $(-0.3, 0.7, 0)$ and (0,1,0)]: (b) SF count rates, (c) NSF count rates. (d) Magnetic signal along diagonal scans at 1.6 K; note that the BG is eliminated through the polarization analysis. Scan paths are not identical, but all run through one $\mathbf{Q}_{IC}$ towards (1,0,0), see (a). The signal in (d)–(g) has been corrected for the magnetic form factor and the Bose factor and represents $\chi''(\mathbf{q}, E)$ convoluted with the resolution function, labelled $\Re * \chi''(\mathbf{q}, E)$. In (e) the results of the scans parallel to the a*/b* axes are shown. Energy scans at $\mathbf{Q}_{IC}$ and $\mathbf{Q}_{FM}$ are shown in (f) and (g), respectively. Lines in (d)–(g) denote the fitted model folded with the resolution. The unfolded incommensurate and QFM susceptibilities are shown in (h) (single component).

TABLE I. (Upper part) Parameters of the $\chi''(\mathbf{q}, E)$ model for Sr_2RuO_4 refined with the polarized INS data for $T = 1.6$ and 150 K. (Lower part) The largest triplet, T, and singlet, S, eigenvalues (in arbitrary units) of the interaction matrices V_s and V_t, respectively [Eq. (3)], obtained for the isotropic susceptibility, $\chi' = \chi'(q, 0)$ or for the anisotropic components χ'_{zz} and χ'_{ab}; the largest eigenvalues for QFM or IC fluctuations only are shown together with those for the total susceptibility.

T [K]	χ'_{FM} [μ_B^2/eV]	W [r.l.u.]	Γ_{FM} [eV]	χ'_{IC} [μ_B^2/eV]	ξ_{IC} [Å]	Γ_{IC} [eV]
1.6	22 ± 1	0.53 ± 0.04	15.5 ± 1.4	213 ± 10	9.7 ± 0.5	11.1 ± 0.8
150	22 ± 2	0.47 ± 0.06	19.0 ± 3.5	89 ± 7	6.1 ± 0.5	17.8 ± 2.9

	QFM T	QFM S	IC T	IC S	total T	total S
χ'	10.6	0.21	16.8	94.8	18	87
χ'_{zz}	11.7	0.23	29.1	164.2	30.3	155.6
χ'_{ab}	9.6	0.19	9.7	54.7	11.3	48.3

dispersion is well known and a lattice dynamical model exists that was used to calculate the phonon signal strength at finite propagation vectors [47,48], while in most cases the $q \to 0$ limit is used as an approximation. Note, however, that the INS signal does not directly correspond to $\chi''(\mathbf{q}, E)$ but to its folding with the resolution function, $\Re * \chi''(\mathbf{q}, E)$, see Figs. 1(d)–(g). Only if the resolution is much better than the typical variation of $\chi''(\mathbf{q}, E)$ the convolution has no visible effect.

The quantitative model fitted to the data consists of two parts: the IC peaks centered at $\mathbf{Q}_{\mathrm{IC}}$ and the broad and weakly $\mathbf{q}$-dependent QFM part at the zone center. We write $\chi''(\mathbf{q}, E) = \chi''_{\mathrm{IC}}(\mathbf{q}, E) + \chi''_{\mathrm{FM}}(\mathbf{q}, E)$, where

$$\chi''_{\mathrm{IC}}(\mathbf{q}, E) = \chi'_{\mathrm{IC}} \frac{\Gamma_{\mathrm{IC}} E}{E^2 + \Gamma_{\mathrm{IC}}^2 [1 + \xi_{\mathrm{IC}}^2 (\frac{2\pi}{a} \Delta q)^2]^2} \qquad (1)$$

is the single-relaxor formula with both $(\Gamma_{\mathbf{q}})^{-1}$ and $\chi'(\mathbf{q}, 0)$ decaying with the same correlation length ξ_{IC}. Here $\Delta q = |\mathbf{q} - \mathbf{q}_{\mathrm{IC}}|$, and is measured in the reciprocal lattice units, (r.l.u.), equal to $2\pi/a$.

Equation (1) describes a typical magnetic response near an AFM instability [51]. The QFM term was described by a broad Gaussian, and its energy dependence in the single-relaxor form with the constant parameter Γ_{FM}:

$$\chi''_{\mathrm{FM}}(q, E) = \chi'_{\mathrm{FM}} \frac{\Gamma_{\mathrm{FM}} E}{E^2 + \Gamma_{\mathrm{FM}}^2} \exp\left(-\frac{q^2}{W^2} 4 \ln(2)\right) \qquad (2)$$

and $\mathbf{q}$ is the distance to the nearest 2D Bragg point. The parameters resulting from a global fit to the whole data set are given in Table I [52]. The model susceptibility was convoluted with the spectrometer resolution using the reslib program package [53] and scaled through phonon scattering [48] yielding the lines in Figs. 1(d)–(g).

The corresponding real part of the susceptibility at zero energy $\chi'(\mathbf{q}, E = 0)$, i.e., the amplitudes of the spectra at fixed $\mathbf{q}$, as well as $\chi''(\mathbf{q}, E)$ for $\mathbf{q}$ along the Brillouin zone diagonal are displayed in Fig. 2. The QFM signal shows no significant anisotropy and corresponds to the macroscopic susceptibility, which also exhibits only weak anisotropy [2,3]. For the IC peak, the model describes the average of the in plane and out of plane susceptibilities [30], with χ'_c (χ'_{ab}) slightly larger (smaller) than this value. The model was obtained by refining the only six parameters with the total set of 120 independent data points at 1.6 K and 76 at 150 K. Thus obtained χ'_{IC} and Γ_{IC} are somewhat higher than those extracted from unpolarized INS [11,26]. The correlation length ξ_{IC} is less accurate but the qualitative decrease at higher temperature is unambiguous. In principle, one should consider the in plane and out of plane components of the IC peak separately and then take their superposition, but the limited statistics does not allow for that. In contrast to the IC signal, the QFM one is basically temperature independent,

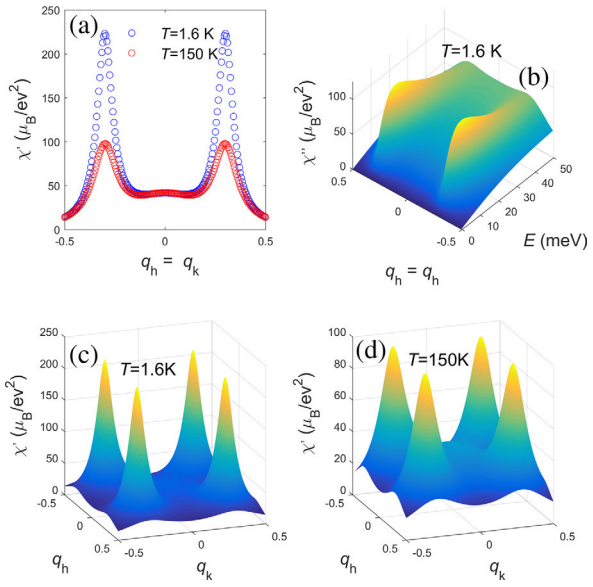

FIG. 2. The real part of the static susceptibility $\chi'(\mathbf{q}, E = 0)$ as described by Eqs. (1) and (2) along the zone diagonal (a) and for the entire zone (c) at 1.6 K and (d) at 150 K; in (b) $\chi''(\mathbf{q}, E)$ is shown along the Brillouin zone diagonal.

which is in agreement with the macroscopic measurement [22]. Thus, the QFM response becomes more visible at high temperatures. Note that, due to the simplicity of the model [52], the macroscopic susceptibility of $\sim 28\mu_B^2/\mathrm{eV(f.u.)}$ is smaller than in the model, $\sim 41\mu_B^2/\mathrm{eV(f.u.)}$.

The model $\chi''(\mathbf{q}, E)$ can also be successfully verified against $1/T_1T$ in NMR [41,42,54–57] and specific heat data [22,58,59], see Supplemental Material [46]. The impact of the QFM fluctuations must not be underestimated; because of the larger phase space, they yield about 85% of the specific-heat enhancement.

The QFM signal in Sr_2RuO_4 does not correspond to the paramagnon scattering expected close to a FM instability [51]; instead it can be viewed as an AFM instability with a small but finite propagation vector near the Brillouin-zone center and a width that largely exceeds the length of the propagation vector. The superposition of several low-$\mathbf{q}$ contributions can result in the observed broad feature centered at $\mathbf{q} = (0, 0)$ and indeed several calculations of the q-dependent susceptibility in Sr_2RuO_4 reveal sharp features near (0.1,0.1,0) associated with the γ band [60–62]. $Ca_{2-x}Sr_2RuO_4$ with $0.2 < x < 0.5$ as well as $Sr_3Ru_2O_7$ exhibit FM or metamagnetic transitions with sizeable moments [44,63]. In these truly FM compounds the magnetic fluctuations also differ from the FM paramagnon response and retain a small q incommensurate AFM character [64–67], although the q width in these materials is much smaller than that of the QFM part in Sr_2RuO_4. The QFM signal in Sr_2RuO_4 exhibits a characteristic energy that is only a little larger than that of the IC signal, supporting the notion that Sr_2RuO_4 is also close to FM order [43,44].

To access the role of the QFM fluctuations in the SC pairing we apply a simple weak-coupling approach relating the spin-mediated pairing interaction $V(\mathbf{k}, \mathbf{k}')$ to the full $\chi(\mathbf{q}, E)$, see, e.g., Ref. [62]: $\lambda\Delta(\mathbf{k}) = \sum_{\mathbf{k}'} V(\mathbf{k}, \mathbf{k}')\Delta(\mathbf{k}')$, where $\Delta(\mathbf{k})$ characterizes the SC order parameter (SOP). $V(\mathbf{k}, \mathbf{k}')$ is, for the singlet and triplet pairings [62]:

$$V_s(\mathbf{q} = \mathbf{k} - \mathbf{k}') = -3I^2(\mathbf{q})\chi'(\mathbf{q}, 0)\frac{1}{\sqrt{v_F(\mathbf{k})v_F(\mathbf{k}')}}$$
$$V_t(\mathbf{q} = \mathbf{k} - \mathbf{k}') = I^2(\mathbf{q})\chi'(\mathbf{q}, 0)\frac{|\hat{\mathbf{v}}_F(\mathbf{k})\hat{\mathbf{v}}_F(\mathbf{k}')|}{\sqrt{v_F(\mathbf{k})v_F(\mathbf{k}')}} \quad (3)$$

where $I(\mathbf{q})$ is defined as $I(q) = \chi_0(\mathbf{q})^{-1} - \chi(\mathbf{q})^{-1}$, and $\chi_0(\mathbf{q})$ is the noninteracting (Lindhardt) susceptibility. Note that only the amplitude of the single-relaxor spectra, $\chi'(\mathbf{q}, 0)$, enters the interaction matrices in this simple model. We use the tight binding Hamiltonian of Ref. [68] and parametrize the interaction as [10]: $I(\mathbf{q}) = I(0)/[1 + b(a/\pi)^2q^2]$, further details are given in the Supplemental Material [46]. The matrices $V_{s,t}(\mathbf{k}, \mathbf{k}')$ are diagonalized by discretizing the Fermi surface into 1301 vectors $\mathbf{k}$. The largest eigenvalue of the interaction matrix defines the solution with the highest critical temperature, and the corresponding eigenvector defines the symmetry and the structure of the SOP. The interaction parameter $I(q)$ is crucial. Based on their calculations for $SrRuO_3$, Mazin and Singh [5,10,69] assigned the q dependence of I to the Hund's rule coupling on oxygen, and estimate $b = 0.08$. In the experiment, we find a much larger value $b = 0.44$, see Fig. 3(a), thus favoring more the triplet pairing.

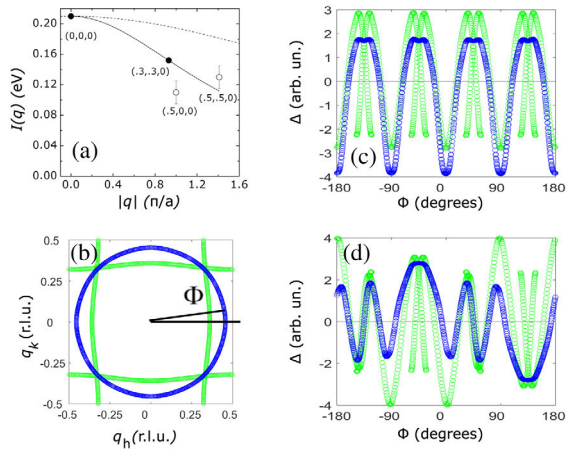

FIG. 3. (a) The interaction $I(\mathbf{q}) = I(0)/[1 + b(a/\pi)^2q^2]$ for $b = 0.08$ (dashed line) and $b = 0.44$ (solid line) compared with the experimental estimates; (b) 2D Fermi surface of Sr_2RuO_4 with the Q1D (green) and Q2D (blue) sheets; (c) and (d) SC order parameter on these sheets plotted against the angle with respect to the k_x axis for the most stable singlet (c) and triplet (d) solutions.

We have diagonalized the matrices described by Eq. (3) using the two contributions separately, and using the total $\chi' = \chi'(\mathbf{q}, 0)$. The results are shown in Table I. As expected, for the IC fluctuations alone singlet solutions are most stable, and the QFM ones give triplets. With the total susceptibility, the IC fluctuations significantly contribute to the triplet solution as well, but the most stable state is still a singlet: the ratio of the largest singlet to the largest triplet eigenvalue is rather high, $R_{s/t} = 4.8$ [52]. Even a five times larger QFM part (clearly incompatible with the experiment) only reduces the ratio to $R_{s/t} = 1.4$. Sharpening the parameter $I(q)$ significantly helps the triplet case, but not enough; tripling b to 1.32 only reduces $R_{s/t}$ to 2.2. Figures 3(c) and 3(d) present the SOPs for the most stable singlet and triplet solutions with the experimental set of parameters. The triplet solution is degenerate with the one rotated by 90°, so that a chiral state can be constructed. Note that both solutions have strong angular anisotropies (even vertical line nodes), not imposed by the p or d symmetries.

We have also estimated the potential effect of matrix elements in various ways [46] and studied the impact of an anisotropic susceptibility, but in all realistic cases the singlet state turned out to be the most instable one. Within simple

spin-fluctuation theory it seems almost impossible to obtain a stable triplet solution even though the QFM signal is much sharper than previously thought.

In conclusion, we have identified the long-sought QFM fluctuations in Sr_2RuO_4, and, by comparing with the phonon scattering, quantitatively determined their amplitude. Combining this QFM signal and the nesting-driven IC response we have constructed the total magnetic susceptibility $\chi''(\mathbf{q}, E)$ at all $\mathbf{q}$, which is consistent with the macroscopic susceptibility, with the specific heat coefficient in the normal state and with the $1/T_1T$ NMR results. Even though the experimentally determined QFM response is stronger and sharper than thought before, the IC component still dominates the spin-fluctuation spectrum in Sr_2RuO_4, so that the total susceptibility favors a singlet order parameter for simple spin-fluctuation mediated pairing. Thus, if the superconductivity in Sr_2RuO_4 is triplet, interactions beyond spin-fluctuation exchange would be required for the pairing mechanism.

This work was supported by the Deutsche Forschungsgemeinschaft (DFG, German Research Foundation)—Project No. 277146847—CRC 1238 (project B04) and by the Japan Society for the Promotion of Science Grants-in-Aid for Scientific Research (KAKENHI) JP15H05852. I. I. M. was supported by Office of Naval Research (ONR) through the Naval Research Laboratory (NRL) basic research program.

*braden@ph2.uni-koeln.de

[1] Y. Maeno, H. Hashimoto, K. Yoshida, S. Nishizaki, T. Fujita, J. G. Bednorz, and F. Lichtenberg, Nature (London) **372**, 532 (1994).
[2] A. P. Mackenzie and Y. Maeno, Rev. Mod. Phys. **75**, 657 (2003).
[3] Y. Maeno, S. Kittaka, T. Nomura, S. Yonezawa, and K. Ishida, J. Phys. Soc. Jpn. **81**, 011009 (2012).
[4] T. M. Rice and M. Sigrist, J. Phys. Condens. Matter **7**, L643 (1995).
[5] I. Mazin and D. Singh, Phys. Rev. Lett. **79**, 733 (1997).
[6] I. I. Mazin and D. J. Singh, Phys. Rev. B **56**, 2556 (1997).
[7] C. Kallin, Rep. Prog. Phys. **75**, 042501 (2012).
[8] C. Kallin and A. Berlinsky, Rep. Prog. Phys. **79**, 054502 (2016).
[9] A. P. Mackenzie, T. Scaffidi, C. W. Hicks, and Y. Maeno, npj Quantum Mater. **2**, 40 (2017).
[10] I. Mazin and D. Singh, Phys. Rev. Lett. **82**, 4324 (1999).
[11] Y. Sidis, M. Braden, P. Bourges, B. Hennion, S. NishiZaki, Y. Maeno, and Y. Mori, Phys. Rev. Lett. **83**, 3320 (1999).
[12] T. Nomura and K. Yamada, J. Phys. Soc. Jpn. **69**, 3678 (2000).
[13] T. Nomura and K. Yamada, J. Phys. Soc. Jpn. **71**, 404 (2002).
[14] S. Raghu, A. Kapitulnik, and S. A. Kivelson, Phys. Rev. Lett. **105**, 136401 (2010).
[15] T. Takimoto, Phys. Rev. B **62**, R14641 (2000).
[16] M. Tsuchiizu, Y. Yamakawa, S. Onari, Y. Ohno, and H. Kontani, Phys. Rev. B **91**, 155103 (2015).
[17] J. W. Huo, T. M. Rice, and F.-C. Zhang, Phys. Rev. Lett. **110**, 167003 (2013).
[18] T. Scaffidi and S. H. Simon, Phys. Rev. Lett. **115**, 087003 (2015).
[19] C. Bergemann, A. Mackenzie, S. Julian, D. Forsythe, and E. Ohmichi, Adv. Phys. **52**, 639 (2003).
[20] C. N. Veenstra, Z.-H. Zhu, M. Raichle, B. M. Ludbrook, A. Nicolaou, B. Slomski, G. Landolt, S. Kittaka, Y. Maeno, J. H. Dil, I. S. Elfimov, M. W. Haverkort, and A. Damascelli, Phys. Rev. Lett. **112**, 127002 (2014).
[21] M. Kim, J. Mravlje, M. Ferrero, O. Parcollet, and A. Georges, Phys. Rev. Lett. **120**, 126401 (2018).
[22] Y. Maeno, K. Yoshida, H. Hashimoto, S. Nishizaki, S-I. Ikeda, M. Nohara, T. Fujita, A. P. Mackenzie, N. E. Hussey, J. G. Bednorz *et al.*, J. Phys. Soc. Jpn. **66**, 1405 (1997).
[23] T. Oguchi, Phys. Rev. B **51**, 1385 (1995).
[24] D. Singh, Phys. Rev. B **52**, 1358 (1995).
[25] I. Hase and Y. Nishihara, J. Phys. Soc. Jpn. **65**, 3957 (1996).
[26] M. Braden, Y. Sidis, P. Bourges, P. Pfeuty, J. Kulda, Z. Mao, and Y. Maeno, Phys. Rev. B **66**, 064522 (2002).
[27] F. Servant, B. Fak, S. Raymond, J. P. Brison, P. Lejay, and J. Flouquet, Phys. Rev. B **65**, 184511 (2002).
[28] A. Liebsch and A. I. Lichtenstein, Phys. Rev. Lett. **84**, 1591 (2000).
[29] J. Mravlje, M. Aichhorn, T. Miyake, K. Haule, G. Kotliar, and A. Georges, Phys. Rev. Lett. **106**, 096401 (2011).
[30] M. Braden, P. Steffens, Y. Sidis, J. Kulda, P. Bourges, S. Hayden, N. Kikugawa, and Y. Maeno, Phys. Rev. Lett. **92**, 097402 (2004).
[31] K. Iida, M. Kofu, N. Katayama, J. Lee, R. Kajimoto, Y. Inamura, M. Nakamura, M. Arai, Y. Yoshida, M. Fujita, K. Yamada, and S.-H. Lee, Phys. Rev. B **84**, 060402(R) (2011).
[32] K. Iida, J. Lee, M. B. Stone, M. Kofu, Y. Yoshida, and S.-H. Lee, J. Phys. Soc. Jpn. **81**, 124710 (2012).
[33] S. Kunkemöller, P. Steffens, P. Link, Y. Sidis, Z. Mao, Y. Maeno, and M. Braden, Phys. Rev. Lett. **118**, 147002 (2017).
[34] M. Minakata and Y. Maeno, Phys. Rev. B **63**, 180504(R) (2001).
[35] M. Braden, O. Friedt, Y. Sidis, P. Bourges, M. Minakata, and Y. Maeno, Phys. Rev. Lett. **88**, 197002 (2002).
[36] J. P. Carlo, T. Goko, I. M. Gat-Malureanu, P. L. Russo, A. T. Savici, A. A. Aczel, G. J. MacDougall, J. A. Rodriguez, T. J. Williams, G. M. Luke, C. R. Wiebe, Y. Yoshida, S. Nakatsuji, Y. Maeno, T. Taniguchi, and Y. J. Uemura, Nat. Mater. **11**, 323 (2012).
[37] S. Kunkemöller, A. A. Nugroho, Y. Sidis, and M. Braden, Phys. Rev. B **89**, 045119 (2014).
[38] M. Sato and M. Kohmoto, J. Phys. Soc. Jpn. **69**, 3505 (2000).
[39] T. Kuwabara and M. Ogata, Phys. Rev. Lett. **85**, 4586 (2000).
[40] K. Kuroki, M. Ogata, R. Arita, and H. Aoki, Phys. Rev. B **63**, 060506(R) (2001).
[41] K. Ishida, H. Mukuda, Y. Kitaoka, Z. Q. Mao, H. Fukazawa, and Y. Maeno, Phys. Rev. B **63**, 060507 (2001).
[42] K. Ishida, H. Mukuda, Y. Minami, Y. Kitaoka, Z. Q. Mao, H. Fukazawa, and Y. Maeno, Phys. Rev. B **64**, 100501 (2001).

[43] J. E. Ortmann, J. Y. Liu, J. Hu, M. Zhu, J. Peng, M. Matsuda, X. Ke, and Z. Q. Mao, Sci. Rep. **3**, 2950 (2013).
[44] S. Nakatsuji, D. Hall, L. Balicas, Z. Fisk, K. Sugahara, M. Yoshioka, and Y. Maeno, Phys. Rev. Lett. **90**, 137202 (2003).
[45] Z. Q. Mao, Y. Maeno, and H. Fukazawa, Mater. Res. Bull. **35**, 1813 (2000).
[46] See Supplemental Material at http://link.aps.org/supplemental/10.1103/PhysRevLett.122.047004 for further information about the polarized INS experiments and about the calculations is given. In addition unpolarized INS data and polarized data at 150 K is presented as well as a quantitative comparison with NMR and specific heat experiments.
[47] M. Braden, W. Reichardt, S. Nishizaki, Y. Mori, and Y. Maeno, Phys. Rev. B **57**, 1236 (1998).
[48] M. Braden, W. Reichardt, Y. Sidis, Z. Mao, and Y. Maeno, Phys. Rev. B **76**, 014505 (2007).
[49] As a result of subtracting similar count rates, the resulting error bars are relatively large (see Fig. 1). The BG contains an essential part that depends only on the scattering angle. By analyzing many **Q** scans, a BG function depending on the scattering angle could be fitted. The variation of the BG also reflects the variation of the NSF count rates indicating that this part of the BG arises from the finite flipping efficiency. Although in the analysis of the magnetic signals, the size of the magnetic scattering has almost exclusively been obtained from the PA, these considerations show that the BG is well understood and properly mastered.
[50] N. Qureshi, P. Steffens, D. Lamago, Y. Sidis, O. Sobolev, R. A. Ewings, L. Harnagea, S. Wurmehl, B. Büchner, and M. Braden, Phys. Rev. B **90**, 144503 (2014).
[51] T. Moriya, *Spin Fluctuations in Itinerant Electron Magnetism* (Springer-Verlag, Berlin, 1985).
[52] The overestimation of $\chi'(0,0)$ seems to arise from the IC Lorentzian tails. The data can be equally well described assuming a Gaussian decay also for the IC amplitude, with the parameters $\chi'_{\mathrm{IC}} = 214\ \mu_B/\mathrm{eV}^2$, $W = 0.12$ r.l.u. and a constant $\Gamma_{\mathrm{IC}} = 11$ meV. With this description there is no contribution of IC parts to $\mathbf{q} = 0$, but the results for the BCS eigenvalue calculation are nearly unchanged. In particular the singlet is still favoured with an eigenvalue (in units of Table I) of 78 compared to 20 for the triplet solution; $R_{s/t} = 3.9$. Note that our analysis together with the macroscopic $\chi'(0,0)$ values excludes an essential high-energy QFM contribution beyond the range of our INS experiments.
[53] A. Zheludev, *ResLib 3.4c* (Oak Ridge National Laboratory, Oak Ridge, TN, 2006).
[54] T. Imai, A. Hunt, K. Thurber, and F. Chou, Phys. Rev. Lett. **81**, 3006 (1998).
[55] C. Berthier, M. H. Julien, M. Horvatić, and Y. Berthier, J. Phys. I (France) **6**, 2205 (1996).
[56] H. Mukuda, K. Ishida, Y. Kitaoka, K. Asayama, Z. Mao, Y. Mori, and Y. Maeno, J. Phys. Soc. Jpn. **67**, 3945 (1998).
[57] K. Ishida, Y. Kitaoka, K. Asayama, S. Ikeda, S. Nishizaki, Y. Maeno, K. Yoshida, and T. Fujita, Phys. Rev. B **56**, R505 (1997).
[58] D. M. Edwards and G. G. Lonzarich, Philos. Mag. **65**, 1185 (1992).
[59] M. Hatatani and T. Moriya, J. Phys. Soc. Jpn. **64**, 3434 (1995).
[60] Q. H. Wang, C. Platt, Y. Yang, C. Honerkamp, F. C. Zhang, W. Hanke, T. M. Rice, and R. Thomale, Europhys. Lett. **104**, 17013 (2013).
[61] L. Boehnke, P. Werner, and F. Lechermann, Europhys. Lett. **122**, 57001 (2018).
[62] I. Eremin, D. Manske, S. G. Ovchinnikov, and J. F. Annett, Ann. Phys. (Amsterdam) **13**, 149 (2004).
[63] R. S. Perry, L. M. Galvin, S. A. Grigera, L. Capogna, A. J. Schofield, A. P. Mackenzie, M. Chiao, S. R. Julian, S. I. Ikeda, S. Nakatsuji, Y. Maeno, and C. Pfleiderer, Phys. Rev. Lett. **86**, 2661 (2001).
[64] O. Friedt, P. Steffens, M. Braden, Y. Sidis, S. Nakatsuji, and Y. Maeno, Phys. Rev. Lett. **93**, 147404 (2004).
[65] P. Steffens, Y. Sidis, P. Link, K. Schmalzl, S. Nakatsuji, Y. Maeno, and M. Braden, Phys. Rev. Lett. **99**, 217402 (2007).
[66] P. Steffens, O. Friedt, Y. Sidis, P. Link, J. Kulda, K. Schmalzl, S. Nakatsuji, and M. Braden, Phys. Rev. B **83**, 054429 (2011).
[67] L. Capogna, E. M. Forgan, S. M. Hayden, A. Wildes, J. A. Duffy, A. P. Mackenzie, R. S. Perry, S. Ikeda, Y. Maeno, and S. P. Brown, Phys. Rev. B **67**, 012504 (2003).
[68] S. Okamoto and A. J. Millis, Phys. Rev. B **70**, 195120 (2004).
[69] I. Mazin and D. Singh, J. Phys. Chem. Solids **59**, 2185 (1998).

Spin fluctuations in Sr_2RuO_4 from polarized neutron scattering: implications for superconductivity
supplemental material

P. Steffens,[1,2] Y. Sidis,[3] J. Kulda,[2] Z. Q. Mao,[4,5,6] Y. Maeno,[4] I. Mazin,[7] and M. Braden[1,*]

[1] *II. Physikalisches Institut, Universität zu Köln, Zülpicher Str. 77, D-50937 Köln, Germany*
[2] *Institut Laue Langevin,71 avenue des Martyrs, 38000 Grenoble, France*
[3] *Laboratoire Léon Brillouin, C.E.A./C.N.R.S., F-91191 Gif-sur-Yvette CEDEX, France*
[4] *Department of Physics, Graduate School of Science, Kyoto University, Kyoto 606-8502, Japan*
[5] *Department of Physics, Tulane University, New Orleans, LA 70118, USA*
[6] *Department of Physics, Pennsylvania State University, University Park, PA 16802, USA*
[7] *Code 6393, Naval Research Laboratory, Washington, District of Columbia 20375, USA*

A. Unpolarized inelastic neutron scattering experiments

We have used the large Sr_2RuO_4 sample also for unpolarized INS experiments on the magnetic fluctuations using the thermal triple-axis spectrometer 2T at the Laboratoire Léon Brillouin. The intensity in the unpolarized experiment is relatively high, but the accessible energy range remains as limited as in the previous triple-axis-spectrometer studies[1,2]. At higher energy it is impossible to discern a broad signal from the background and phonon scattering. Figure S1 shows a scan that passes more than an entire diagonal of the Brillouin zone, thereby crossing the ferromagnetic wave vectors (-1,0,0) and (0,1,0), the incommensurate peaks at (-0.7,0.3,0) and (-0.3,0.7,0) and the antiferromagnetic zone boundary (-.5,.5,0). There are well pronounced maxima at each of these positions. Only by comparison with the data from the polarized experiment described in the main text, one can decide, which of these signals have magnetic origin. For this purpose, the data for the SF channel and its sum with the nSF channel are, after multiplication with an appropriate scale factor, overlayed to the unpolarized data. As this data has been taken with the neutron spin polarization parallel to the scattering vector, any magnetic scattering is contained in the SF channel. It proves that the intensity at (-0.5,0.5,0) is entirely non-magnetic. It can be explained with the soft phonon mode occurring at this Brillouin zone boundary[3,4]. Also, the strongest part of the intensity near $\mathbf{Q}_{FM}$=(±1,0,0) is non-magnetic and can be attributed to phonon scattering. The phonon dispersion[3,4] shows that the lowest longitudinal branch in [ξ 0 0] direction ends at a rather low energy of ∼8 meV at (1,0,0). Similar **Q** positions like (2,1,0) and (3,0,0) further prove the non-magnetic character of the strong and sharp signal. Concerning the nesting signals, the data in Fig. S1 fully confirm previous experiments and again indicate a shoulder at the small q side in agreement with reference[2]. The scattering observed in reference[5] around the (0,0,2) Bragg point can also be attributed to phonon scattering.

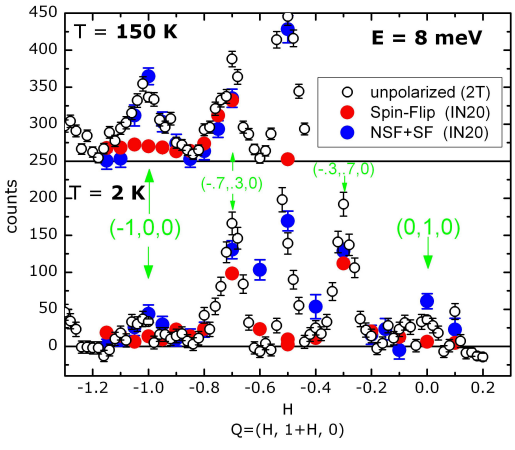

FIG. S1: Diagonal scans at 8 meV at 2 and 150 K recorded with unpolarized neutrons. The open symbols have been measured with unpolarized neutrons on 2T; by use of polarized neutrons (IN20, H||Q) it is possible to distinguish the magnetic or non-magnetic character of the various peaks.

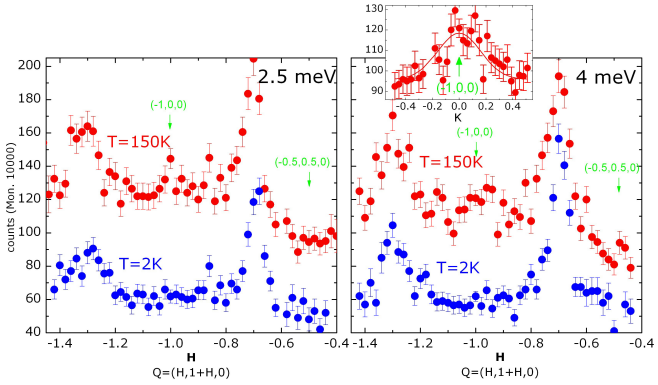

FIG. S2: Diagonal scan with unpolarized neutrons at 2.5 and 4 meV (original count rate, no background correction, no offset). Inset: transverse scan across (-1,0,0) at T=150 K.

At lower energy transfer one may exclude phonon contributions (except acoustic phonons near the Γ point). Figure S2 shows diagonal scans at two such energy transfers, 2.5 and 4 meV, at low and high temperature. Compared to the scan at higher energy the strong peak at (-

0.5,0.5,0) has completely disappeared in accordance with the temperature dependence and energy of the rotation mode[3,4], and also the relatively sharp signal at $\mathbf{Q}_{FM}$ is suppressed. The two incommensurate peaks are clearly visible, and the left one at (-1.3,-0.3,0) is weakened by a factor ∼2.5 compared to the right one at (-0.7,0.3,0) following the magnetic form factor of Ru. Around (-1,0,0), there is clearly higher intensity than at (-0.5,0.5,0), especially at T=150 K, and the transverse scan at 4 meV and 150 K (inset) supports this statement. While this is an indication for the presence of a broad signal around $\mathbf{Q}_{FM}$ and confirms the intensity map and the comparable scans in Ref. 2, these unpolarized data do not unambiguously indicate a magnetic origin, and a quantitative assessment is impossible due to the uncertain background. Note, however, that the background besides spurious and phonon scattering decreases with the scattering angle and thus with $|\mathbf{Q}|$, so that the background around (-1,0,0) should be lower than that at (-0.5,0.5,0).

B. Polarized INS experiments

Polarized INS experiments were performed on the spectrometer IN20 at the Institut Laue Langevin using focussing Heusler monochromator and analyzer crystals in zickzack configuration. A set of Helmholtz coils were used to guide the neutron polarization at the sample, and the sufficient strength of guide fields was achieved at each scan position by rotating the Helmholtz coils. A pyrolithic graphite filter was used to suppress higher order contamination and all scans were performed with constant final energy, k_f=4.1$\mathring{A}^{-1}$. We worked in the [100]/[010] scattering plane, because the relaxed vertical-Q resolution optimally integrates the q2D magnetic signals in this case. Measurements were performed in the first and second Brillouin zone of the 2D lattice. Therefore the Q range is limited and the correction with the simple Ru form factor is appropriate.

Figure S3 shows the results of polarized diagonal scans at 150 K presenting the total magnetic scattering corresponding to two components of the generalized susceptibility. Compared to the low-temperature data the FM response becomes much more visible, because the IC fluctuations are strongly suppressed with temperature while the qFM signal is almost temperature independent, as it is well reflected in the modeling of the total susceptibility.

C. Quantitative comparison with NMR results

The fitted model of the total spin susceptibility may be quantitatively compared to measurements of nuclear magnetic resonance (NMR). The NMR technique also probes the magnetic fluctuations by determining the spin-lattice relaxation rate $\frac{1}{T_1}$ of the nuclear magnetization. When divided by the temperature T, it can be expressed as[6]:

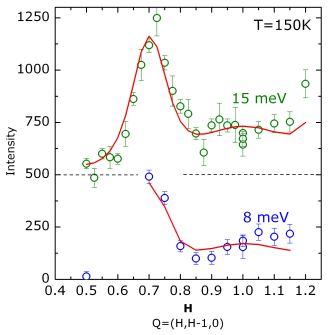

FIG. S3: Magnetic signal corresponding to the sum of in-plane and out-of-plane componens at 150 K along diagonal scans passing through the IC and FM positions. The presentation is similar to that in Figure 1. Data at 15 meV are shifted by 500 counts.

$$\frac{1}{T_1T} = \frac{k_B\gamma_N^2}{(g\mu_B)^2}\sum_q |A(q)|^2 \frac{\chi''(q,\omega)}{\omega} \qquad (1)$$

Here, γ_N is the gyromagnetic ratio for the nucleusand $A(q)$ is the hyperfine coupling. Values of $\gamma_N/2\pi$ are 2.193 MHz/T for ^{101}Ru and 5.772 MHz/T for ^{17}O[7]. The hyperfine coupling can depend on Q and on the polarization of the fluctuation. For ^{101}Ru we use $A(q) = -250\text{kOe}/\mu_B$[8,9], independent of q. For ^{17}O, $A(q)$ is q-dependent and vanishes at q=(0.5,0.5,0) for geometric reasons on the (in-plane) O(1) site. The form $|A(q)|^2 = A^2[1 + \frac{1}{2}(cos(q_h a) + cos(q_k b))]$ has been suggested[10] with $A = -18.5$ or $-28.8\text{kOe}/\mu_B$ depending on the polarization[7]. Similar to neutron scattering, different components of χ'' have to be summed up (those perpendicular to the field). This allows a determination of anisotropies, as for instance in Reference[11]. In equation (1) the direction sum is not explicitly included; for an isotropic case a factor 2 has to be added.

As the typical resonance frequencies are in the range of MHz and thus by far lower than the characteristic energy scales, NMR probes the limit $\omega \to 0$ with respect to neutron scattering (ω's of the order THz). The obtained values for $\frac{1}{T_1T}$ are thus simply the Brillouin zone average of the frequency derivative of $\chi'(q)/\Gamma_q$ weighted by the hyperfine fields.

A series of NMR measurements on both ^{17}O and ^{101}Ru have been carried out[8,10–12]. They find a temperature dependent signal which increases by a factor 2-3 between room temperature and low temperature. It has been shown[1,11] that the absolute increase of the signal reflects the temperature dependence of the contribution from the incommensurate peaks. In addition, there seems to be a temperature-independent offset which has been ascribed to ferromagnetic fluctuations. Qualitatively, this agrees with our polarized-neutron results, because the broad ferromagnetic component does not change as function of temperature, in contrast to the incommensurate one, see

TABLE S1: Brillouin zone averages of the magnetic fluctuations $\sum_q \chi''(q,\omega)/\omega$ in Sr_2RuO_4 (sum of in-plane and out-of-plane component); first value plain average, second value weighted with the $(1+\frac{1}{2}(cos(q_h a)+cos(q_k b)))$ term. The results are given in $\frac{\mu_B^2}{\mathrm{eV}}\mathrm{meV}^{-1}$. The two last columns are the NMR $1/\mathrm{T_1T}$ relaxation rates in $\mathrm{s}^{-1}\mathrm{K}^{-1}$ under the assumption ^{101}A=250kOe/μ_B and ^{17}A=33kOe/μ_B. The experimental results for $^{101}1/\mathrm{T_1T}$ are 14.5 and 8 $\mathrm{s}^{-1}\mathrm{K}^{-1}$ and for $^{17}1/\mathrm{T_1T}$ 0.77 and 0.42 $\mathrm{s}^{-1}\mathrm{K}^{-1}$ at 1.6 and 150 K, respectively[12].

1.6 K			$^{101}1/\mathrm{T_1T}$	$^{17}1/\mathrm{T_1T}$
FM	840	1180	5.6	0.33
IC	1840	1350	12.2	0.38
Sum	2680	2530	17.8	0.71
150 K				
FM	730	1030	4.9	0.29
IC	1140	880	7.6	0.25
Sum	1870	1910	12.4	0.53

Table SI.

For a quantitative comparison, the averages over the Brillouin zone in the zero frequency limit, $\sum_q \chi''(q,\omega)/\omega$, can straightforwardly be evaluated. The results are given in $\frac{\mu_B^2}{\mathrm{eV}}\mathrm{meV}^{-1}$ in Table I and underline the importance of the ferromagnetic contribution for the understanding of the NMR data. When comparing the so obtained values for the NMR relaxation rates with the measured values[12], one finds good agreement with the ^{17}O data and a small overestimation for the ^{101}Ru data. In particular, the contribution of the FM part to $1/\mathrm{T_1T}$ is also quantitatively in good agreement to the temperature-independent part.

This relatively good quantitative agreement with the NMR data strongly supports the correctness of the model for $\chi''(q,E)$ and the conclusions inferred from the inelastic neutron scattering experiments.

D. Quantitative comparison with specific-heat data

Another quantitative verification of the model can be made with the low-temperature specific heat coefficient γ, which has been determined in the normal state to amount to 37.5 $\mathrm{mJ/molK}^2$ [13]. The spin-fluctuation contribution to the specific-heat coefficient per formula unit can be estimated by the average of the reciprocal characteristic energy[14,15]:

$$\gamma_{SF} = \frac{\pi k_B^2}{N} \sum_q \frac{1}{\Gamma_q}. \qquad (2)$$

Using the parameters in Table I (main text), one can make a simple estimation by assuming Γ to be constant in cylinders that have the diameter of the $\mathbf{q}$ width of the fluctuation similar to the analysis for metamagnetic $Ca_{2-x}Sr_xRuO_4$[16,17], which exhibits a very strong enhancement of the Sommerfeld coefficient. For the four incommensurate peaks with small extension in reciprocal space ($\Delta q \sim 0.1$ r.l.u.), the total contribution amounts to only about 6 $\mathrm{mJ/mol{\cdot}K}^2$ (or slightly more when using a smaller Γ_{IC}). The broad ferromagnetic component contributes about 32 $\mathrm{mJ/mol{\cdot}K}^2$. The sum is in excellent agreement with the macroscopic value. It is remarkable that the contribution of the broad ferromagnetic fluctuations is by far the dominant one, because ferromagnetic fluctuations cover a much wider region in $\mathbf{q}$ space.

E. Solving linearized BCS gap equations

In order to access quantitatively potential of the measured magnetic fluctuations as mediators for the superconducting pairing, we incorporated the magnetic susceptibility into the linearized BCS gap equations. First, we parameterized the Fermi surface using the tight-binding model of Ref.[18]. We solved a 2D gap problem, thereby neglecting any k_z dependence, and discretized the 2D Fermi surface using points separated by a distance of 0.005 reduced lattice units. In order to avoid artificial violation of the tetragonal symmetry this sampling was doubled by exchanging k_x and k_y. In total, the Fermi-surface vector contained 1301 (k_x, k_y) points: 396 on the xz, 396 on the yz and 509 on the xy sheet, respectively.

The interaction matrix $V(\mathbf{k},\mathbf{k}')$ describing the pair scattering between two points on the Fermi surface $\mathbf{k}$ and $\mathbf{k}'$ is given by equation (3) of the main text. Note that $V(\mathbf{k},\mathbf{k}')$ is different for the triplet and singlet cases. In particular, there is an angular factor between the Fermi velocities entering the triplet matrix elements, see, e.g. Ref.[19]. Otherwise $V(\mathbf{k},\mathbf{k}')$ is given by the observed susceptibility and the q dependent interaction function $I(q)$, which is also used in RPA analyses of susceptibility. Solving the gap equation $\lambda\Delta(\mathbf{k}) = \sum_{\mathbf{k}'} V(\mathbf{k},\mathbf{k}')\cdot\Delta(\mathbf{k}')$, where $\Delta(\mathbf{k})$ is the amplitude of the SC order parameter (SOP), amounts to calculating the eigenvalues of the matrix $V(\mathbf{k},\mathbf{k}')$. The largest eigenvalue determines the transition temperature of the first superconducting instability. Note that we did not attempt to calculate the prefactor determining the absolute value of the critical temperature, but, rather, concentrated on the *relative* stabilities of the most favorable singlet and triplet solutions. The eigenvector of a particular solution of Eq. 3 determined the structure (not in the absolute units, but up to a temperature-dependent constant) of the SOP just below the transition. at lower temperature the structure of SOP may deviate from this solution, since Eq. 3 represents the the *linearized* BCS problem. This structure includes the angular dependence of the SOP and can be visualized by plotting it against the polar angle, i.e. the angle between (k_x, k_y) and (1,0), for each Fermi-surface sheet.

Then, we calculate the ratio of the largest singlet to largest triplet eigenvalues, $R_{s/t}$, which gauges the relative stability of the singlet vs. triplet state. If the two are close, one can imagine that refinement of the model can

tip the balance toward one or the other parity. As we discussed in the main text, this is not the case and singlet states are always much more stable.

Using the fitted model parameters of the susceptibility in Table I of the main text and with the interaction function obtained from the experiment with b=0.44 we find a singlet state to be most instable, $R_{s/t}$=4.8. The eigenvectors for this state, as well as for the most unstable triplet state, are shown in Fig. 3 of the main text. Enhancing the FM contribution by a factor two and five reduces this ratio to 3.7 and 1.4, respectively, but so strong FM components are incompatible with the INS data. Also, enhancing the q dependence of the interaction by using b=0.88 and 1.32 in the interaction function, results in smaller $R_{s/t}$ values of 3.6 and 2.2, respectively, still very far from any possibility of a triplet solution. Therefore, varying the parameters even well beyond what can be considered to be in accordance with the experiment does not qualitatively change the preponderance of the singlet solution.

We have also estimated a potential effect of matrix elements in Eq. (3) by retaining only the intra-orbital pairing, as suggested in Ref.[24], or only interactions within the q1D and the q2D bands, but in either case the singlet solution remains much more stable than the triplet one. Applying the total susceptibility to the γ band only results in a largely favored singlet state, $R_{s/t}$=3.5. Magnetic anisotropy favors the triplet state[20–22] by reducing the factor 3 in the fist line of eq. 3. The macroscopic susceptibility tells us that the qFM part has an easy-axis anisotropy of 20% . For the IC part, INS finds a larger anisotropy, of about a factor of two[23]; NMR places an upper limit at a factor of three[11]. Using the latter, we find the numbers shown in Table I. A chiral state with $\mathbf{d}||\mathbf{z}$ would have triplet-pair spins aligned in the xy plane, and thus be disadvantaged compared to a spin-isotropic singlet state; the ratio rises to $R_{s/t}$ =7.7. A planar state with spins perpendicular to the planes will benefit from the easy-axis anisotropy, but not enough: the $R_{s/t}$ is still 2.9.

* e-mail: braden@ph2.uni-koeln.de

[1] Y. Sidis, M. Braden, P. Bourges, B. Hennion, S. NishiZaki, Y. Maeno, and Y. Mori, Phys. Rev. Lett. **83**, 3320 (1999).
[2] M. Braden, Y. Sidis, P. Bourges, P. Pfeuty, J. Kulda, Z. Mao,and Y. Maeno, Phys. Rev. B **66**, 064522 (2002).
[3] M. Braden, W. Reichardt, S. Nishizaki, Y. Mori, and Y. Maeno, Phys. Rev. B **57**, 1236 (1998).
[4] M. Braden, W. Reichardt, Y. Sidis, Z. Mao, and Y. Maeno, Physical Review B **76**, 014505 (2007).
[5] K. Iida, J. Lee, M. B. Stone, M. Kofu, Y. Yoshida, and S.-H. Lee, J. of Phys. Soc. Jpn. **81**, 124710 (2012).
[6] T. Moriya, *Spin Fluctuations in Itinerant Electron Magnetism* (Springer-Verlag Berlin Heidelberg, 1985).
[7] H. Mukuda, K. Ishida, Y. Kitaoka, K. Asayama, Z. Mao, Y. Mori, and Y. Maeno, J. Phys. Soc. Japan **67**, 3945 (1998).
[8] K. Ishida, H. Mukuda, Y. Kitaoka, Z. Q. Mao, H. Fukazawa, and Y. Maeno, Phys. Rev. B **63**, 060507 (2001).
[9] K. Ishida, Y. Kitaoka, K. Asayama, S. Ikeda, S. Nishizaki, Y. Maeno, K. Yoshida, and T. Fujita, Phys. Rev. B **56**, R505 (1997).
[10] C. Berthier, M. Julien, M. Horvati, and Y. Berthier, J. Phys. I France **6**, 2205 (1996).
[11] K. Ishida, H. Mukuda, Y. Minami, Y. Kitaoka, Z. Q. Mao, H. Fukazawa, and Y. Maeno, Phys. Rev. B **64**, 100501 (2001).
[12] T. Imai, A. Hunt, K. Thurber, and F. Chou, Phys. Rev. Lett. **81**, 3006 (1998).
[13] Y. Maeno, K. Yoshida, H. Hashimoto, S. Nishizaki, S-I. Ikeda, M. Nohara, T. Fujita, A. P. Mackenzie, N. E. Hussey, J. G. Bednorz, et al., J. Phys. Soc. Japan **66**, 1405 (1997).
[14] D. M. Edwards and G. G. Lonzarich, Philosophical Magazine **65**, 1185 (1992).
[15] M. Hatatani and T. Moriya, J. Phys. Soc. Japan **64**, 3434 (1995).
[16] O. Friedt, P. Steffens, M. Braden, Y. Sidis, S. Nakatsuji, and Y. Maeno, Phys. Rev. Lett. **93**, 147404 (2004).
[17] P. Steffens, O. Friedt, Y. Sidis, P. Link, J. Kulda, K. Schmalzl, S. Nakatsuji, and M. Braden, Phys. Rev. B **83**, 054429 (2011).
[18] S. Okamoto and A. J. Millis, Phys. Rev. B **70**, 195120 (2004).
[19] I. Eremin, D. Manske, S. G. Ovchinnikov, and J. F. Annett, Ann. Phys. **13**, 149 (2004).
[20] M. Sato and M. Kohmoto, J. of Phys. Soc. Jpn. **69**, 3505 (2000).
[21] T. Kuwabara and M. Ogata, Phys. Rev. Lett. **85**, 4586 (2000).
[22] K. Kuroki, M. Ogata, R. Arita, and H. Aoki, Phys. Rev. B **63**, 060506(R) (2001).
[23] M. Braden, P. Steffens, Y. Sidis, J. Kulda, P. Bourges, S. Hayden, N. Kikugawa, and Y. Maeno, Phys. Rev. Lett. **92**, 097402 (2004).
[24] T. M. Rice and M. Sigrist, J. Phys. Condens. Matter **7**, L643 (1995).